TÜBİTAK

Turkish Journal of Earth Sciences

http://journals.tubitak.gov.tr/earth/

Research Article

Turkish J Earth Sci
(2020) 29: 579-595
© TÜBİTAK
doi:10.3906/yer-1905-21

In situ magnetic susceptibility and gamma radiation data in the Candela-Monclova intrusive belt, Northeast Mexico: case studies of the Cerro Colorado and Cerro Marcelinos plutons

José Alberto BATISTA RODRÍGUEZ*, Edgar Niño RODRÍGUEZ, Pedro Antonio RODRÍGUEZ RIOJAS, Roberto DÍAZ MARTÍNEZ, Antonio RODRÍGUEZ VEGA, Felipe de Jesús LÓPEZ SAUCEDO
Higher School of Engineering, Autonomous of University Coahuila, Saltillo, Mexico

Received: 30.05.2019 • **Accepted/Published Online:** 25.01.2020 • **Final Version:** 05.05.2020

Abstract: The Cerro Marcelinos (CM) and Cerro Colorado (CC) plutons are part of the Candela-Monclova intrusive belt (NE Mexico), which is mid-Eocene in age (43–35 Ma). It intrudes into the Sabinas Basin, primarily made up of limestones, of Lower and Upper Cretaceous age. Around several intrusions, including the CM and CC plutons, mineralizations are known. However, how much hidden mineralizations would occur is not known. Trends within the plutons and in contact aureoles are also poorly described at present. Therefore, we provide here in situ magnetic susceptibility (MS) and gamma ray spectrometry (GS) data along two composite transects, one in each pluton, to delineate such potential trends. The data show variations of 0.003×10^{-3} SI and 104×10^{-3} in MS and of 7.1 nGy/h and 196 nGy/h in GS with a clear relation to rock type and amount of metasomatism. The radioactive contents in the outcrops of contact metamorphic rocks indicate a contact metasomatism with differing degrees of alteration during emplacement of the plutons. The host limestones have magnetic minerals incorporated during the intrusion process. MS and GS indicate an increase in the degree of acidity towards the center of both plutons, possibly associated with the later stages of the magmatic differentiation process. The MS could divide the igneous rocks into two groups, weakly magnetic (group 1 with MS $\leq 3 \times 10^{-3}$ SI) and strongly magnetic (group 2 with MS $> 3 \times 10^{-3}$ SI), associated with the magnetite and ilmenite series, respectively. These classes provide useful information regarding the internal magnetic zoning in the plutons, which can be associated with mineralizations of mainly Au and Cu. Mainly, the magnetite series (group 2) delimited more perspective zones for mineral exploration. This zoning in MS could guide future mineral exploration in both plutons.

Key words: Candela-Monclova intrusive belt, Cerro Colorado pluton, Cerro Marcelinos pluton, magnetic susceptibility, gamma spectrometry

1. Introduction

The geology of northeastern Mexico is characterized by several magmatic events, during which many intrusions were emplaced. The Sabinas Basin is one of the main structures resulting from this geological evolution (Wilson, 1990; Goldhammer, 1999). The Laramide orogeny (Late Cretaceous to Paleogene) and younger events of extensional nature in the region were responsible for the sedimentary sequence of this basin, with folding and emplacement of numerous intrusions of different compositions and ages. The Candela-Monclova Intrusive Belt (CMIB, Figure 1) formed in the mid-Eocene and is associated with different types of mineralization (Sewell, 1968; Chavez-Cabello et al., 2011). Our understanding of some of the intrusions is still incomplete, in particular the Cerro Colorado (CC) and Cerro Marcelinos (CM) plutons (Figure 1). Polymetallic deposits of Fe, Cu, Zn, Au, and Ag are linked with these two plutons (Santiago-Carrasco et al., 2001; SGM, 2005). Evidence is still required about their internal zonation due to magmatic differentiation, alteration intensity of host rocks, and the magmatic rocks themselves that generate a contact metamorphism (contact aureole), as well as the tectonic setting of both plutons and host rocks.

Magnetic susceptibility (MS) and natural gamma radioactivity (NGR) are two physical properties directly related to the mineralogical composition of rocks (Brimhal and Adams, 1969; Clark, 1997; Harenyama et al., 2006). MS is mainly related to the content, distribution, types, and characteristics of magnetic minerals (Clark, 1997), whereas NGR is related to the mineralogical composition of the rocks (Dickson and Scott, 1997). Processes related to the genesis and emplacement of intrusions determine their mineralogical compositions and, therefore, the

* Correspondence: josebatista@uadec.edu.mx

This work is licensed under a Creative Commons Attribution 4.0 International License.

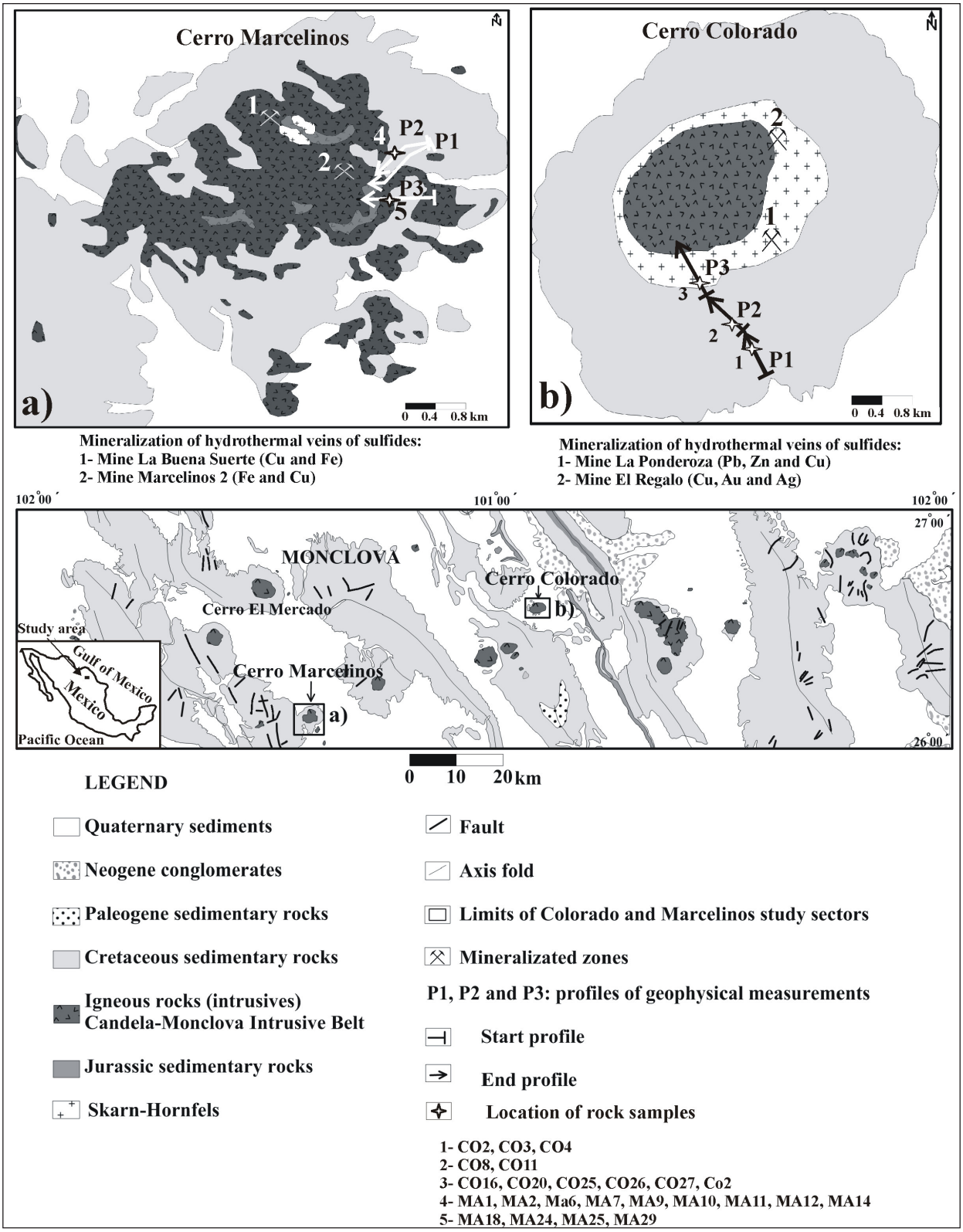

Figure 1. The Candela-Monclova intrusive belt (modified from González-Ramos et al., 2008). a) Enlargement of the Cerro Marcelinos (CM) pluton (modified from Santiago-Carrasco et al., 2001). b) Enlargement of the Cerro Colorado (CC) pluton (modified from SGM, 2005). Detailed locations of the samples are given in Figures 10 and 11.

values of MS and NGR (Dickson and Scott, 1997; Aydin et al., 2007; Oliveira et al., 2008; Maulana et al., 2013). In this research, in situ measurements of MS and GS of the CC and CM plutons are reported and used as a proxy of the main characteristics of both intrusives.

2. Geological setting

The CMIB is located in Northeast Mexico in the Sabinas Basin (Figure 1). This basin originated in the Late Triassic-Middle Jurassic during the opening of the Gulf of Mexico, due to the fragmentation of the Pangea supercontinent (Padilla and Sánchez, 1986; Wilson, 1990; Goldhammer, 1999). During the origin and evolution of this basin, magmatism resulted in igneous rocks of many types and ages. The CMIB is one such example of the intrusion of these rocks during the Eocene and is composed of monzonites, quartz-monzonites, quartz-diorites, monzodiorites, and, to a lesser extent, granodiorites, diorites, and granites. This intrusive belt has an E-W orientation and comprises sixteen intrusions (Figure 1; Sewell, 1968; Chávez-Cabello et al., 2009). Most of these intrusions are formed of subvolcanic rocks with porphyritic textures, with the exception of the Cerro El Mercado. All the igneous rocks are metaluminous, indicating great affinity with granites generated in volcanic arcs (I-type granites) above the subduction zone. The CC and CM rocks exhibit enrichment of incompatible elements, such as Rb, Ba, and Th (Chávez-Cabello et al., 2009). The abundance of trace elements in these rocks suggests that they were formed from magmas generated by partial melting of the mantle during the subduction of an oceanic plate (Farallon Plate) beneath North America (Chávez-Cabello et al., 2009). During magmatism, Mesozoic sedimentary rocks were folded, fractured, and altered by metasomatic and hydrothermal processes successively (SGM, 2005).

Both plutons, CM and CC, are composed of granodiorites and diorites that intrude rocks of Cretaceous sedimentary formations (mainly limestones), generating contact metamorphism and producing hornfels (Santiago-Carrasco et al., 2001; SGM, 2005).

The plutons are found as stocks, dykes, and sills. In the CM, the contact aureole has mineralized veins, in which silicification and oxidation of Fe are observed, as well as garnet and Cu carbonates (malachite and azurite). These characteristics imply possible skarn deposits of Fe and Cu at depth (Santiago-Carrasco et al., 2001). At the CC, the contact zone between igneous and sedimentary rocks (contact aureole) exhibits oxidation, argillization, silicification, and epidotization. These processes are associated with the formations of Cu-Fe skarn deposits with subordinate values of Au and Mo. In this contact aureole the mineralization appears disseminated or in veins inside the cornean rocks. The mineralogy includes pyrite, pyrrhotite, traces of chalcopyrite, bornite, malachite, azurite, pyrolusite, magnetite, specularite, hematite, limonite, quartz, and calcite (SGM, 2005).

3. Acquisition and processing of data

In situ measurements of MS and NGR were carried out at 164 outcrops of igneous, sedimentary (limestone), and metamorphic rocks (belonging to contact metamorphism aureole). These outcrops are located in three transects in the CC pluton and in the CM pluton (Figure 1). This latter physical property of the rocks is obtained through gamma spectrometry (GS) measurements emitted by the radioactive isotope K^{40} and radioactive isotopes of the U^{238}, U^{235}, and Th^{232} series (Dickson and Scott, 1997).

Using a geological map at a scale of 1:50,000 taken from Santiago-Carrasco et al. (2001) and SGM (2005), the transects are located to cut the plutons and their host rocks (Figure 1). Five measurements of the MS were taken at each sampling location using a KT-10 Plus magnetic susceptibility meter manufactured by Terraplus Inc. This instrument has a maximum sensitivity of 1×10^{-6} SI units and a measurement range of 0.001×10^{-3} to 9999.99×10^{-3} SI units on smooth surfaces for MS measurements. Note that these measurements do not provide volume MS, only a relative measurement. The susceptibility meter was placed directly on the rock, on a relatively flat surface of the rock, because MS measurements are significantly affected by the flatness of the measurement surface as 95% of the signal is integrated in the first 3 cm (Lecoanet et al., 1999). Therefore it is necessary to make the measurements on a surface as flat as possible. Generally, those surfaces do not show visible signs of weathering. The GS was measured on the rock face directly with a RS-125 portable gamma-ray spectrometer manufactured by Radiation Solutions Inc., which has four channels that record: total gamma intensity (nGy/h), concentrations of potassium (K in %), equivalent uranium (eU in ppm), and equivalent thorium (eTh in ppm). Potassium concentrations are obtained from the peak of K^{40}, while uranium and thorium concentrations are estimated from radioactive isotopes of the U^{238}, U^{235}, and Th^{232} series. For this reason, the term "equivalent" or its abbreviation "e" is used to indicate uranium concentrations (eU) estimated from the U^{238} and U^{235} series, as well as thorium concentrations (eTh) estimated from the Th^{232} series. This spectrometer has high sensitivity with a large 2.0×2.0 NaI crystal of 103 cm^3, which allows high detection efficiency and takes readout in % of K and ppm of U and Th. One measurement of GS was performed for 120 s at each sampling location. Rock samples were collected at various sampling locations of the studied transects based on the MS and GS values. Petrographic analysis was performed on thin-section and polished surfaces to assess the main minerals of the rocks, including those that

contribute most to the values obtained from MS and GS. All data obtained were statistically processed, calculating minimum, maximum, geometric mean, and histograms of the dataset, as well as the geometric mean and standard deviation in each igneous rock group. In the calculation of the histograms, two class intervals ($MS \leq 3 \times 10^{-3}$ SI and $MS > 3 \times 10^{-3}$ SI) were selected to classify mainly the igneous rocks as weakly magnetic and strongly magnetic (Clark, 1997; Oniku et al., 2008). The weakly magnetic igneous rocks will be associated with the ilmenites series and the strongly magnetic igneous rocks will be associated with the magnetite series (Ishihara, 1977; Ishihara et al., 2000; Maulana et al., 2013). A joint interpretation of the geophysical data with the geological and petrographic information was carried out.

4. Results

Throughout the studied transects, there are outcrops of igneous and metamorphic rocks not reported on the geological maps at the 1:50,000 scale taken as the basis for this research (Santiago-Carrasco et al., 2001; SGM, 2005). Therefore, CC and CM plutons have a greater spatial distribution than that shown on the geological maps (Figure 1). For these reasons, there are igneous rock outcrops in all transects.

Previous studies of both plutons (Santiago-Carrasco et al., 2001; SGM, 2005) reported that the geological characteristics observed along the transects are also found in other areas of them. Therefore, it is possible to characterize each pluton using three one-dimensional transects.

Along the transects of both plutons all rocks are fractured and weathered (Figures 2a–2d and 3a–3d). In the igneous rocks, these processes are observed mainly towards the borders of plutons (Figures 2b, 2c, 3b, and 3c). The fracture density of the igneous, sedimentary, and metamorphic rocks enabled in situ MS measurements of the nonfractured sections of these rocks to be taken.

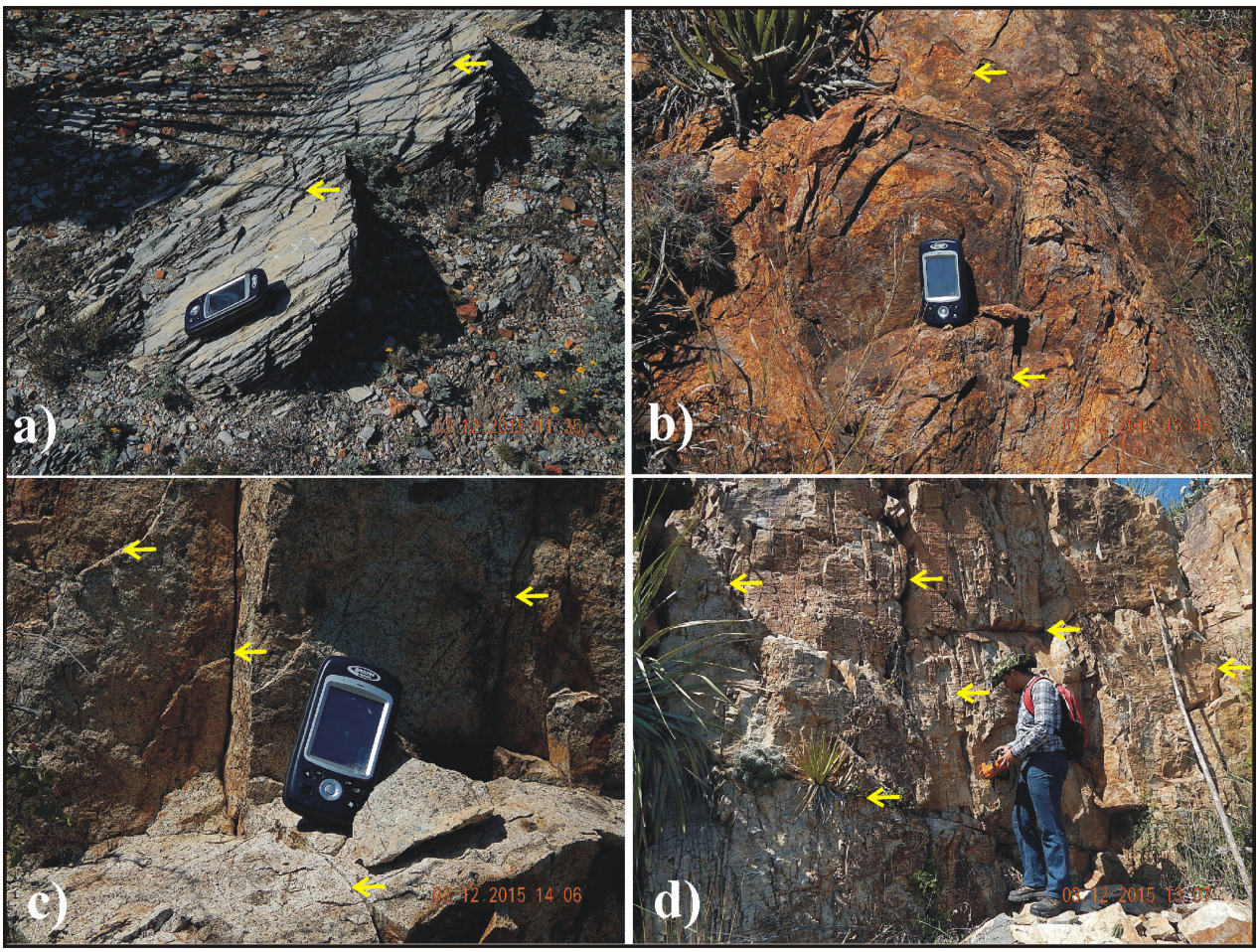

Figure 2. The CC pluton. a) Fractured carbonated rocks with laminar appearance. b) Intrusive rock with intense chemical weathering. c) Fractured intrusive rocks with light chemical weathering. d) Fractured metamorphic rocks with light chemical weathering. Yellow arrows indicate fractures.

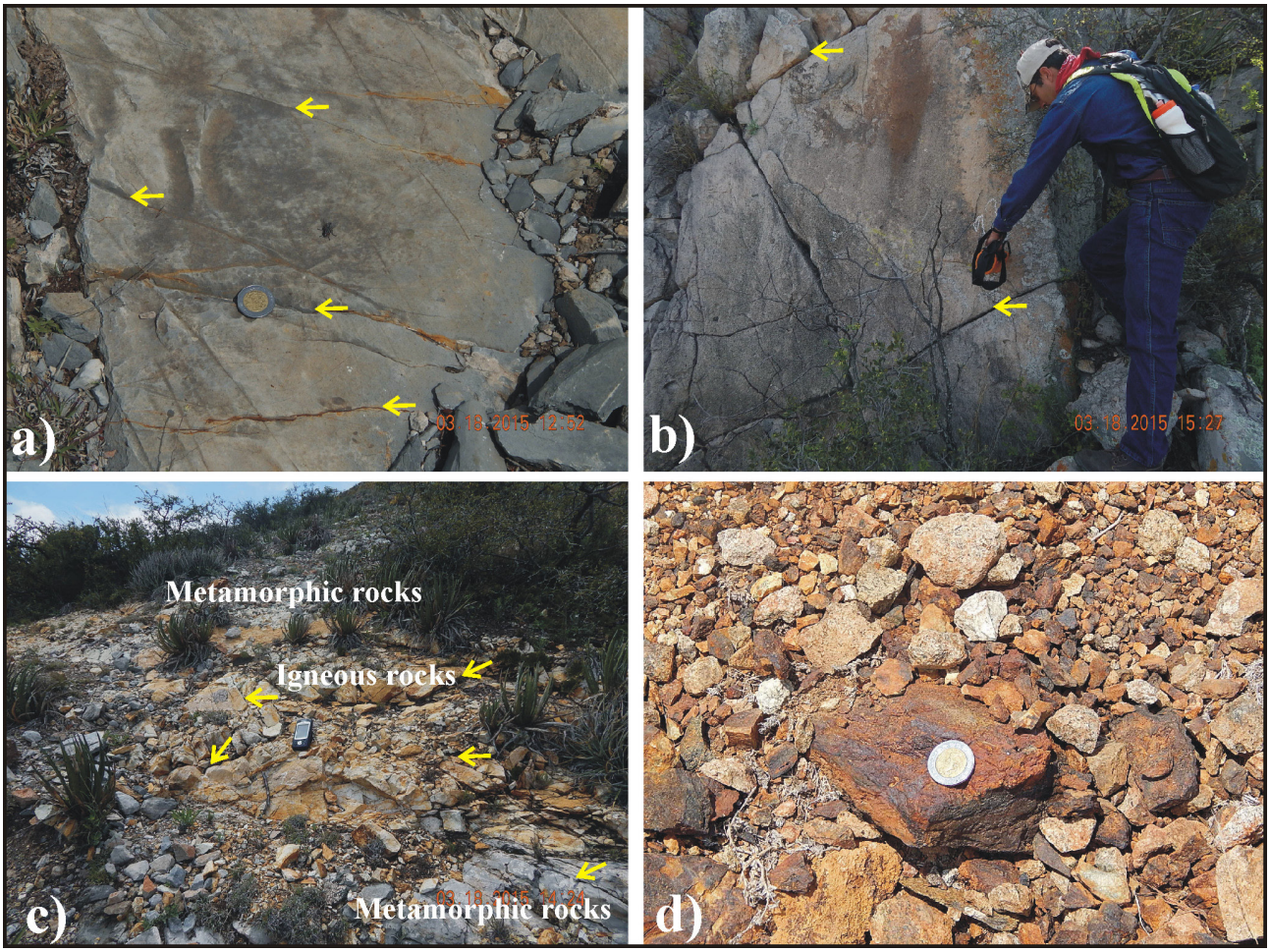

Figure 3. The CM pluton. a) Carbonated rocks with fissures filled with Fe oxides and hydroxides, b) large blocks of intrusive rocks, c) highly fractured igneous rocks within metamorphic rocks, d) Fe mineralization. Yellow arrows indicate fractures.

The igneous rocks also show some mineralized zones, mainly rich in Fe oxides and hydroxides (Figures 2b and 3d). Similarly, petrographic analysis also indicates these minerals in other rocks (Figures 4–9).

4.1. Cerro Colorado pluton

4.1.1. Igneous rocks

The macroscopic analysis of igneous rocks suggests that in the CC pluton the igneous rocks can be granodiorites or diorites according to Chávez-Cabello et al. (2009). Analysis of thin sections and polished surfaces does not allow classification of these rocks, but it indicates that the igneous rocks of this pluton are composed mainly of phenocrysts of plagioclase and small crystals of pyrite and Fe oxides and hydroxides (Figures 4 and 6).

4.1.1.1. Magnetic susceptibility (MS)

MS in both plutons exhibits a wide variability from 0.003 to 104×10^{-3} SI (Table; Figures 10 and 11), which is consistent with the range of studied rocks (igneous, sedimentary, and metamorphic rocks). The igneous rocks have the highest values. In the CC pluton, these rocks have MS from 0.1 to 40×10^{-3} SI with a geometric mean of 1.58×10^{-3} SI (Figure 10). Such values can be controlled by both paramagnetic and ferromagnetic minerals (Clark, 1997) such as iron sulfides, iron oxides, and hydroxides according to sample analysis (Figure 4, 6, 7, 8, and 9). The greatest variation in MS is observed in igneous rocks (see the geometric standard deviation in the Table), in which large differences are found not only between the sampling locations but also within a single location of a rock block (Figure 2c), e.g., sampling location 13 (P13) in transect 3 of the CC pluton (Figure 10).

At the edges of both plutons, the rocks have relatively low MS values, sometimes comparable with those of the host limestone (Figures 10 and 11). The values and variations of MS increase towards the inside of the plutons. Specifically, the area covered by transect 2 in the CC pluton (Figure 10) shows the greatest variation in the MS of the

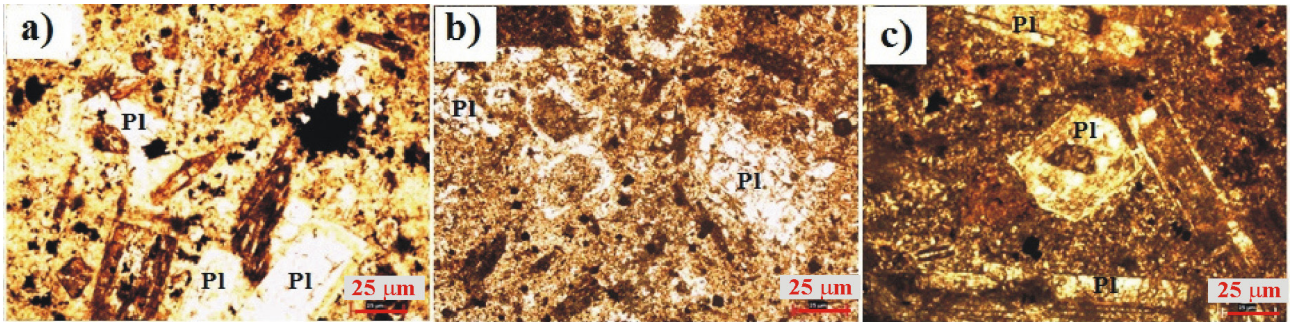

Figure 4. Images of thin sections of intrusive rocks located in CC pluton. Photomicrographs from: a) CO2 sample in transect 1 (P1), b) CO8 sample and c) CO11 sample in transect 2 (P2) shown under transmitted light without analyzer. Dark colors indicate iron oxide minerals, and Pl indicates plagioclase.

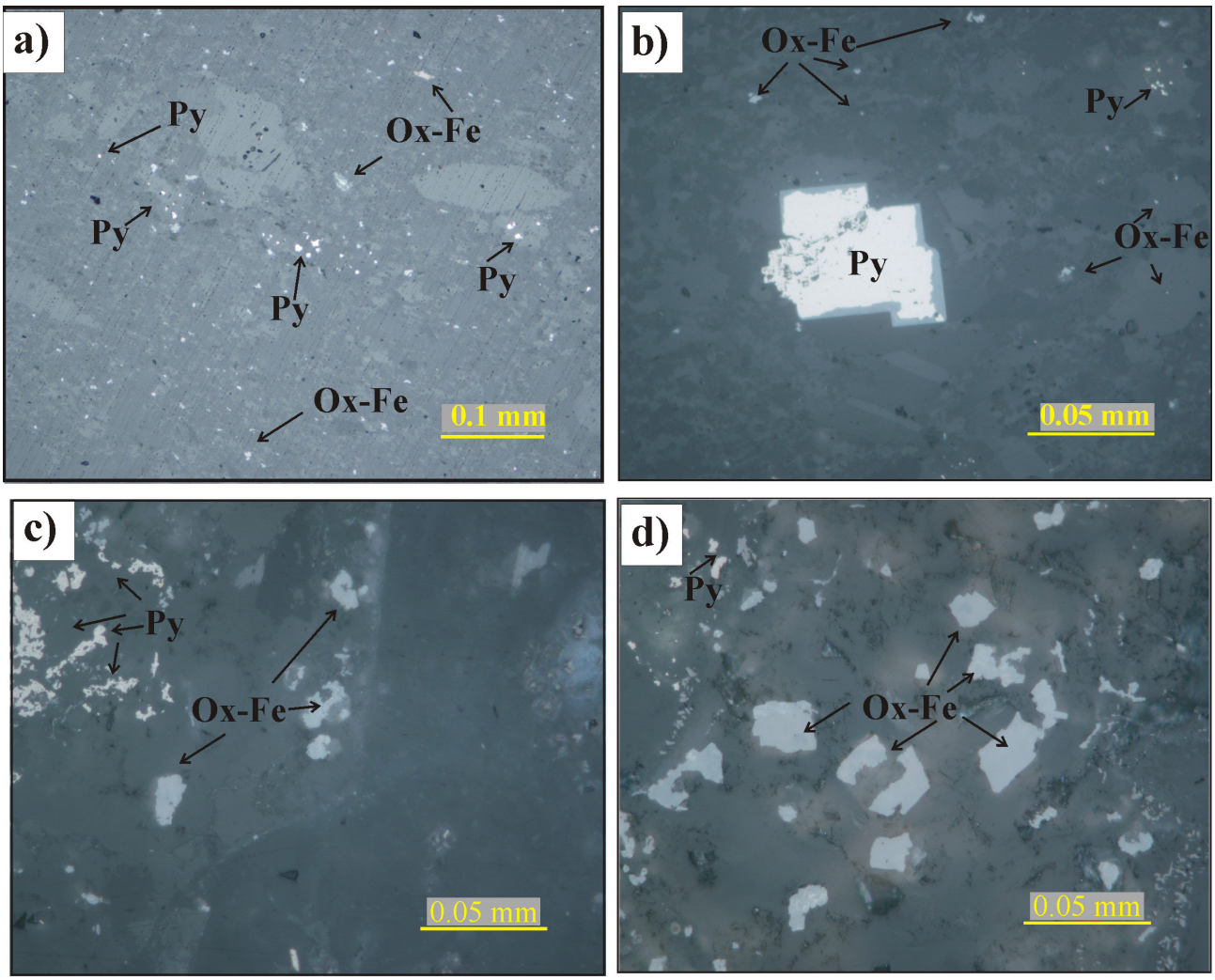

Figure 5. Reflected light images of thin sections of sedimentary rocks located in CC pluton. Transect 1 (P1). a, b) Photomicrographs from the limestone close to the pluton (taken from Batista-Rodríguez et al., 2017). c, d) Photomicrographs of igneous rock shown under reflected light without analyzer. Py indicates pyrite, Ox-Fe indicates iron oxides. CO3 and CO4 indicate sample numbers.

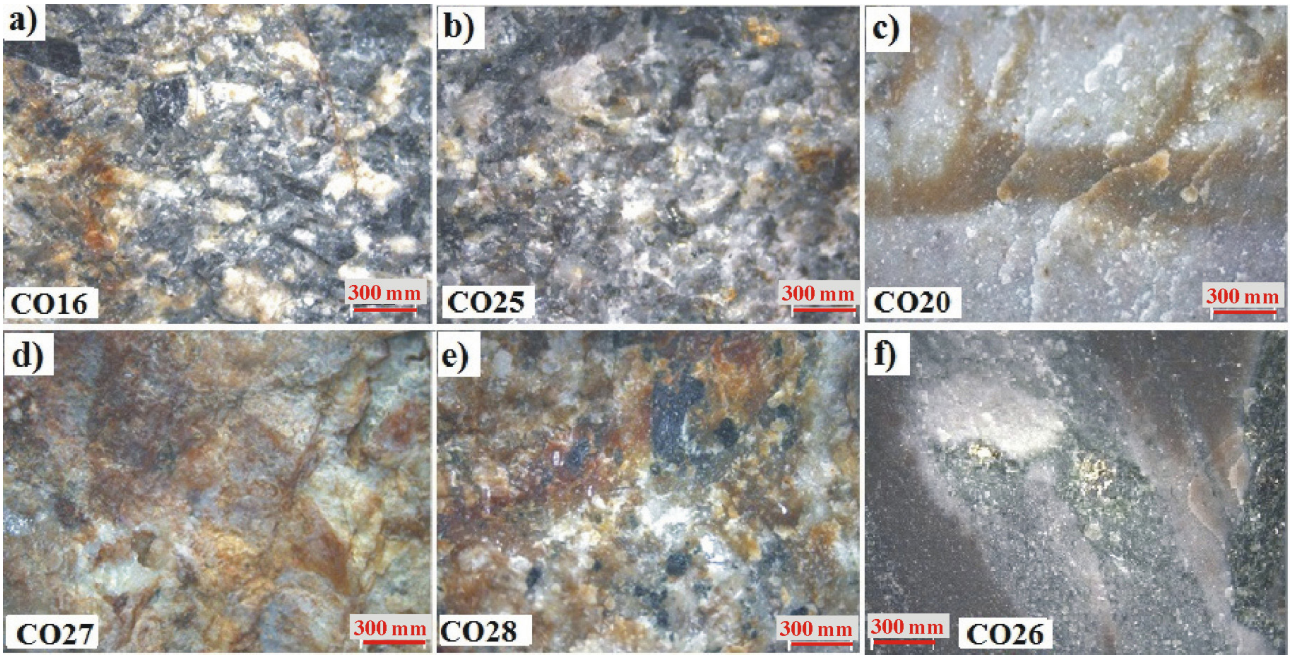

Figure 6. Low-magnification binocular images of rocks located in the CC pluton. Transect 3 (P3). a, b, d, e) Igneous rocks. c, f) Metamorphic rocks. CO16 to CO28 indicate sample numbers. Dark colors indicate iron oxide and hydroxide minerals.

igneous rocks. These variations are related to the changes in magnetic mineral content in these rocks. For example, samples CO8 and CO11 are both taken from this zone, with sample CO11 presenting higher iron oxide mineral content (Figure 4b and 4c). This area is located close to the contact metasomatism zone (Figure 1), which in the fieldwork shows a larger area than the one shown on the geological map of the CC pluton (SGM, 2005).

Within the CC pluton in transect 3 (Figures 1 and 10), the MS tends to decrease in both magnitude and range variability, thus indicating a possible decrease in magnetic mineral content. Petrographic analysis indicates a decrease in the content of these minerals in rocks with lower MS values. The CO25 sample is taken in igneous rocks with higher values, unlike the CO27 and CO28 samples. The first sample shows greater enrichment in iron oxide minerals, according to its dark gray colors (Figure 6b). The other two samples should be more enriched in iron hydroxide minerals (brown color; Figures 6d and 6e), with less magnetic minerals.

The MS values of igneous rocks in the CC pluton show a bimodal distribution (Figure 12), which is typical of these rocks due to low MS values of rocks dominated by paramagnetic minerals, with high MS values for rocks dominated by ferromagnetic minerals, such as magnetite, hematite, and pyrrhotite (Clark, 1997; Oniku et al., 2008). Thin-section analysis of samples of the CC pluton indicates iron oxide minerals, possibly magnetite, as well as pyrite and iron hydroxide minerals (Figures 4, 6a, 6b, 6d, and 6e).

Based on the MS values, the igneous rocks of both plutons are classified into two groups (group 1: MS $\leq 3 \times 10^{-3}$ SI and group 2: MS $> 3 \times 10^{-3}$ SI; Figures 10, 11, and 12). The igneous rocks belonging to group 1 are classified as weakly magnetic, whereas those of group 2 are classified as strongly magnetic (Clark, 1997; Oniku et al., 2008).

According to this classification, we conclude that the principal magnetic carriers of group 1 rocks could be paramagnetic minerals, such as ferromagnesian silicates, Fe sulfides, etc. (Oniku et al., 2008). For the igneous rocks of group 2, the principal magnetic carriers could be ferro/ferrimagnetic minerals, such as magnetite, titanomagnetite, pyrrhotite, and ilmenite (Clark, 1997; Oniku et al., 2008).

The analysis of the MS histograms of the two plutons (Figure 12) indicates that group 1 also includes all sedimentary and metamorphic rocks and represents 65% of the measurements on various types of igneous rocks. Therefore, group 2 in both plutons only includes 35% of the measurements in these rocks.

4.1.1.2. Gamma ray spectrometry (GS)

GS values have a wide variation along the transects in both plutons (Table; Figures 13 and 14). The eU, eTh, and K contents are different in each rock type and outcrop studied. The igneous rocks of the CC pluton have K content from 1.1% to 4.2% with a geometric mean of 2%, eU content from 0.4 to 4.9 ppm with a geometric mean of 1.85 ppm, and eTh content from 3.7 to 11 ppm with a geometric mean of 6.4 ppm. In these rocks, the GS total

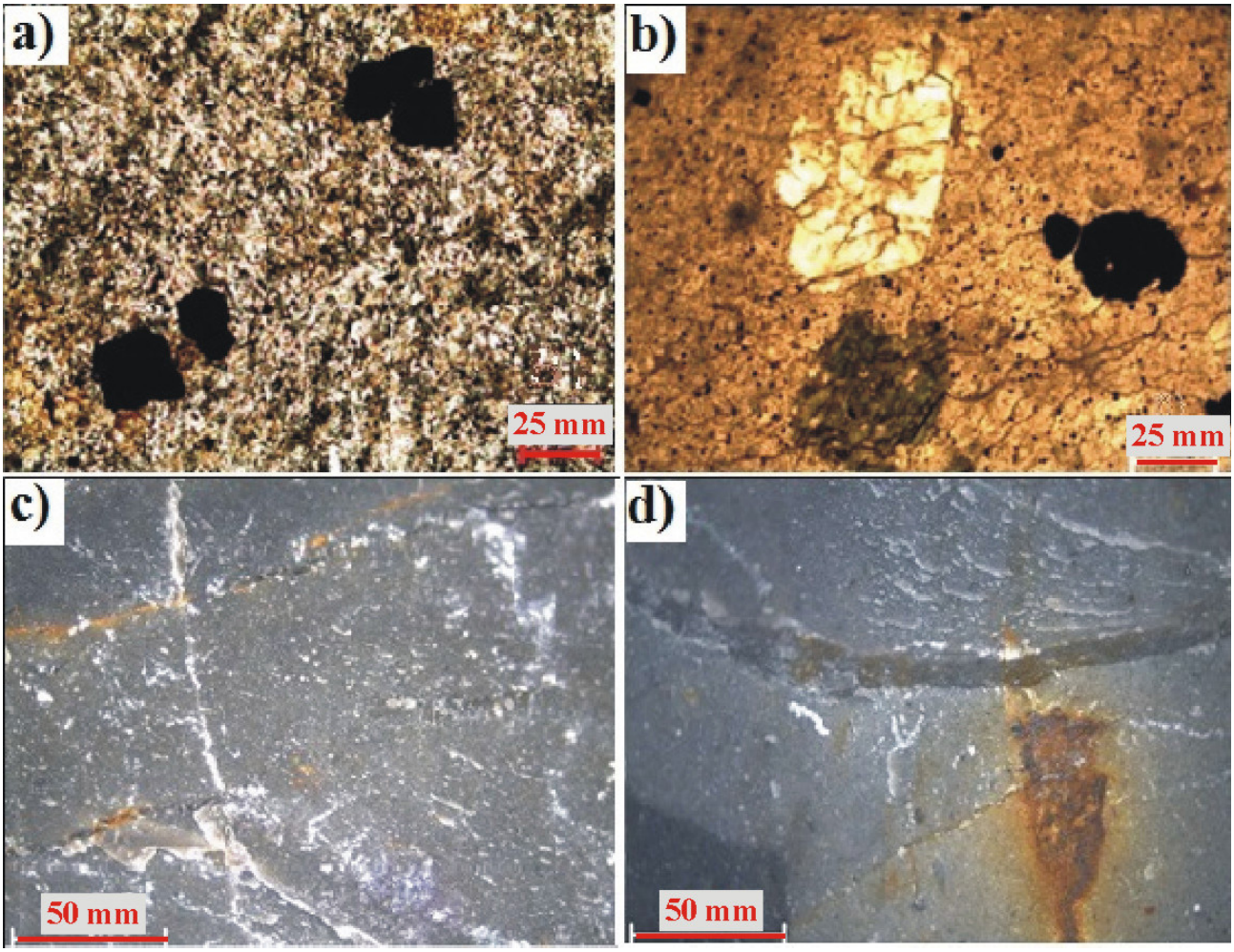

Figure 7. Images of rocks located in CM pluton. Transect 1 (P1). Photomicrographs of intrusive rocks: a) MA6 sample and b) MA14 sample shown under transmitted light without analyzer. Dark colors indicate iron oxide minerals. Low-magnification binocular images of a limestone rock: c, d) MA2 sample. Brown color indicates iron oxide and hydroxide minerals.

values, as well as the eU, eTh, and K contents, increase towards the inside of plutons (Figures 13).

4.1.2. Sedimentary rocks

In the CC pluton the host sedimentary rocks sometimes show comprehensive degrees of metamorphism (Figure 2a) and have pyrite with rectangular faces (Figure 5; Batista-Rodríguez et al., 2017), as well as iron oxides and hydroxides (Figures 5, 7c, and 7d).

4.1.2.1. Magnetic susceptibility (MS)

Generally, the sedimentary rocks in both plutons have the lowest MS values (Table; Figures 10 and 11), which suggests that MS is carried mainly by paramagnetic minerals (Carmichael, 1989). In the CC pluton these rocks have MS from 0.03 to 0.55 × 10^{-3} SI with a geometric mean of 0.21 × 10^{-3} SI (Table; Figures 10).

In both plutons, the outcrops of sedimentary rocks show marked differences in MS values (Figures 10 and 11). For example, the sedimentary rocks of transect 1 of the CC pluton have lower MS that these same rocks located in transects 2 and 3, closer to the center of the pluton. The increase in the MS values of the sedimentary rocks should be linked to their enrichment in iron oxides during the emplacement of the intrusives. This is evidenced in thin-section analysis of the limestone sample (CO23 sample; Figures 5a and 5b) taken in transect 1 of the CC pluton (Figure 10).

4.1.2.2. Gamma ray spectrometry (GS)

The sedimentary rocks of the CC pluton have K content from 0.5% to 1.6% with a geometric mean of 1.0%, eU content from 1.5 to 4.5 ppm with a geometric mean of 2.7 ppm, and eTh content from 2.1 to 6.8 ppm with a geometric mean of 4.5 ppm (Table). These rocks are more radioactive than those of the CM pluton and generally are more enriched in eU and eTh. According to the eTh/eU ratio, the eU increases more than the eTh.

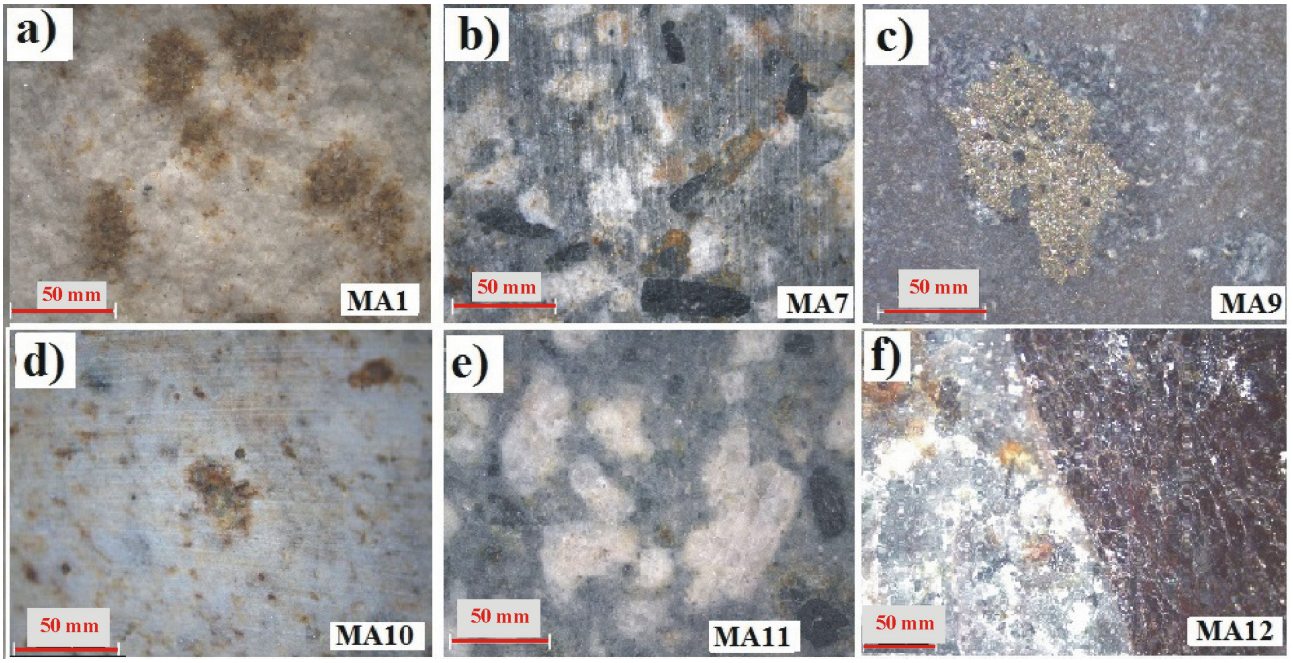

Figure 8. Low-magnification binocular images of intrusive rocks located in CM pluton. Transect 2 (P2). Dark colors indicate iron oxide and hydroxide minerals.

4.1.3. Metamorphic rocks

In the CC pluton, these rocks are fractured, forming blocks with different dimensions (Figure 2d). Dark colors indicate iron oxides and hydroxides minerals (Figures 6c and 6f).

In this contact metasomatism zone of the CC pluton the metamorphic rocks can present MS values relatively similar to some igneous rocks (Figure 10), indicating their enrichment in magnetic minerals. For example, the CO20 sample of metamorphic rock has dark colors that suggest iron oxides and hydroxides minerals (Figure 6c).

4.1.3.1. Magnetic susceptibility (MS)

The metamorphic rocks in the CC pluton have MS from 0.43 to 0.91 × 10^{-3} SI with a geometric mean of 0.66 × 10^{-3} SI (Table; Figures 10), suggesting magnetic carriers similar to those of sedimentary rocks (paramagnetic minerals).

4.1.3.2. Gamma ray spectrometry (GS)

In the CC pluton, the metamorphic rocks have higher contents of the radioactive elements and are more radioactive than those of the CM pluton. These rocks have K content from 1.5% to 4.6% with a geometric mean of 2.3%, eU content from 1.1 to 5.2 ppm with a geometric mean of 3.0 ppm, and eTh content from 5.7 to 14 ppm with a geometric mean of 10 ppm (Table).

4.2. Cerro Marcelinos pluton

4.2.1. Igneous rocks

According to Chávez-Cabello et al. (2009), the igneous rocks in the CM pluton may also be granodiorites or diorites rocks, which are also mainly composed of plagioclase phenocrysts, small pyrite crystals, and Fe oxides and hydroxides (Figures 7, 8, and 9).

4.2.1.1. Magnetic susceptibility (MS)

In the CM pluton, the igneous rocks have MS from 0.01 to 104 × 10^{-3} SI with a geometric mean of 1.1 × 10^{-3} SI (Table; Figure 11), indicating that this physical property can be controlled by both paramagnetic and ferromagnetic minerals. In this pluton, variations of MS values are often related to variation in the color of the blocks (Figure 11c). For example, red blocks have higher MS values than gray ones. According to the microscopic analysis of a sample taken from a red block (MA25 sample), the higher MS values are related to iron oxide and hydroxide (Figure 9c).

The intermediate areas of the three transects in the CM pluton show the greatest variation in the MS of the igneous rocks. These variations can be related to the changes in iron oxide and hydroxide mineral contents, according to changes in dark colors of the MA6, MA7, and MA9 samples (Figures 7, 8b, and 8c). These areas are located close to a contact metasomatism zone observed in the fieldwork. This zone is not shown on the geological map due to its scale (Santiago-Carrasco et al., 2001).

At the outer end of the three transects in the CM pluton (Figures 1 and 11), MS shows a tendency to decrease in magnitude and range variability. Petrographic analysis indicates a decrease in the magnetic mineral contents of rocks with lower MS values. The MA11 sample was taken

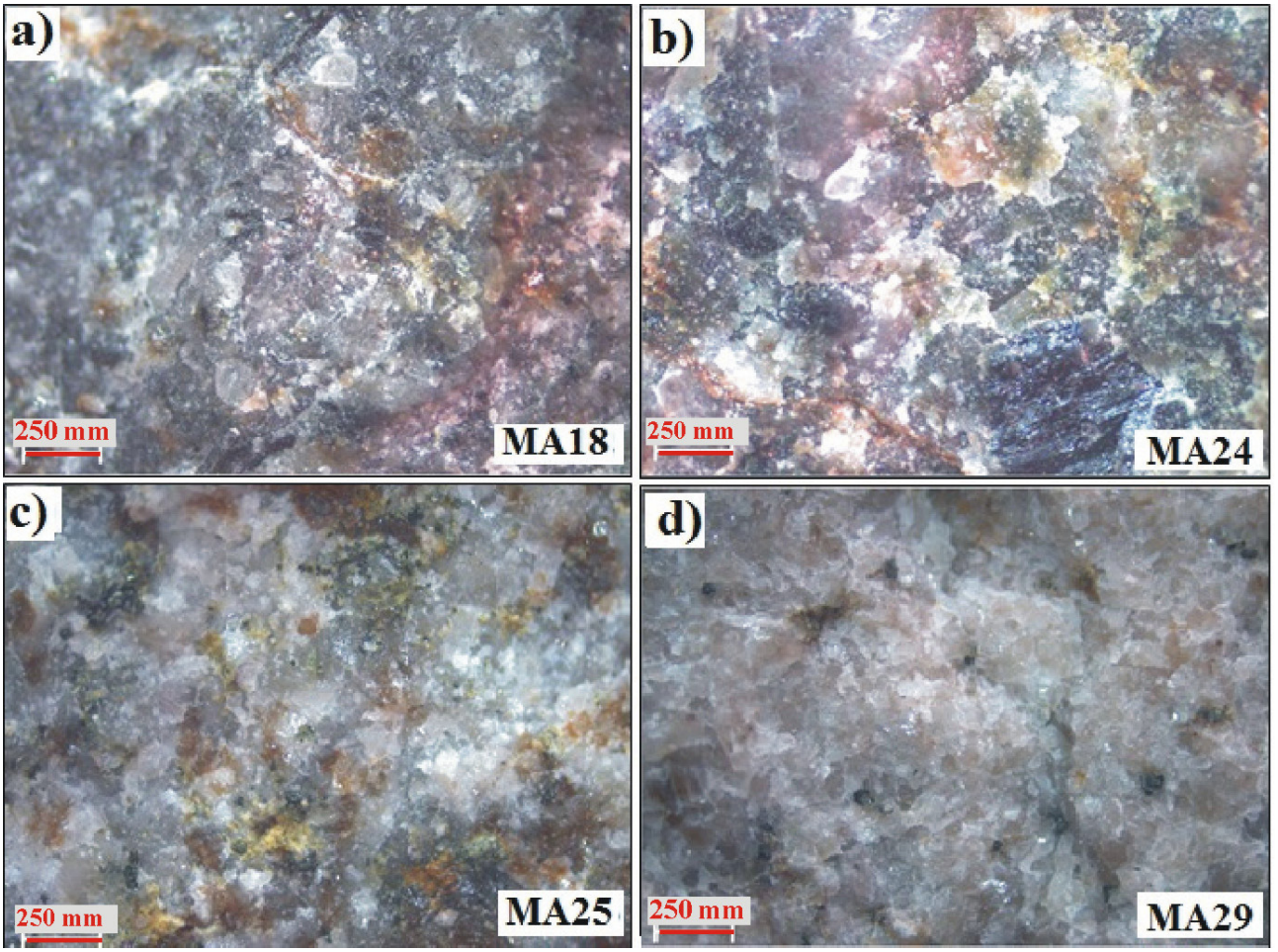

Figure 9. Low-magnification binocular images of intrusive rocks located in CM pluton. Transect 3 (P3). Dark colors indicate iron oxide and hydroxides mineral.

from igneous rocks with higher values than the MA12 and MA29 samples. The first sample has more enrichment in iron oxide minerals (Figures 8e, 9d, and 9f).

The bimodal distribution of the MS values of igneous rocks in CM plutons (Figure 12) can be related to iron oxide minerals, possibly magnetite, as well as pyrite and iron hydroxide minerals, detected in thin-section analysis (Figures 7a, 7b, 8, and 9).

4.2.1.2. Gamma ray spectrometry (GS)

The igneous rocks of the CM pluton have higher contents of the radioactive elements and are more radioactive than those of the CC pluton. These rocks have K content from 1.2% to 6% with a geometric mean of 2.5%, eU content from 0.6 to 9.1 ppm with a geometric mean of 2.3 ppm, and eTh content from 4.3 to 30 ppm with a geometric mean of 9.3 ppm.

The GS total values, as well as the eU, eTh, and K contents, also increase towards the inside of pluton (transect 3 in Figure 14). The petrographic analysis of four samples of transect 3 (Figure 14), suggests an increase in the content of the felsic minerals of the rocks (possibly SiO_2 rich minerals; Figure 9) towards the inside of the pluton.

4.2.2. Sedimentary rocks

The host sedimentary rocks in the CM pluton are enriched in Fe oxides and hydroxides (Figures 3a, 7c, and 7d). These host sedimentary rocks have higher values of MS than those of the CC pluton, with MS from 0.003 to 0.59 × 10^{-3} SI and a geometric mean of 0.05 × 10^{-3} SI (Table; Figure 11). These rocks also have K content from 0% to 3.3% with a geometric mean of 1.0%, eU content from 0 to 6.9 ppm with a geometric mean of 0.3 ppm, and eTh content from 0 to 16 ppm with a geometric mean of 1.6 ppm.

4.2.3. Metamorphic rocks

Within the metamorphic rocks of the CM pluton there are small injections of intrusions (Figure 3c). These rocks have lower magnetic values than the sedimentary rocks, with MS from 0.01 to 0.21 × 10^{-3} SI and a geometric mean of 0.06 × 10^{-3} SI (Table; Figure 11). Also, these rocks have K

Table. Descriptive statistics of in situ measurements of MS ($\times 10^{-3}$ SI) and GS in rocks of the CC and CM plutons. N1, N2, and N3: Number of MS measurements in igneous, metamorphic, and sedimentary rocks, respectively. M1, M2, and M3: Number of GS measurements in igneous, metamorphic, and sedimentary rocks, respectively. Min., Max., and M.: Minimum, maximum, and geometric mean, respectively. R: eTh/eU.

Cerro Colorado pluton																		
	Igneous rocks						Metamorphic rocks						Sedimentary rocks (limestones)					
	MS	It	K	eU	eTh	R	MS	It	K	eU	eTh	R	MS	It	K	eU	eTh	R
Min.	0.1	35	1.1	0.4	3.7	1.5	0.43	58	1.5	1.1	5.7	1.2	0.03	28	0.5	1.5	2.1	0.7
Max.	40	101	4.2	4.9	11	11	0.91	110	4.6	5.2	14	11	0.55	53	1.6	4.5	6.8	3.5
M.	1.58	54	2	1.85	6.4	3.4	0.66	80	2.3	3.0	10	3.4	0.21	41	1	2.7	4.5	1.7
Cerro Marcelinos pluton																		
Min.	0.01	41	1.2	0.6	4.3	1.5	0.01	13	0.2	0.8	1	0.6	0.003	7.1	0	0	0	0
Max.	104	196	6	9.1	30	15	0.21	31	0.5	2	5.4	5.6	0.59	143	3.3	6.9	16	10
M.	1.1	81	2.5	2.3	9.3	3.1	0.06	21	0.3	1.4	3.6	2	0.05	22	1	0.3	1.6	3

It (nGy/h), K (%), eU (ppm), and eTh (ppm).
CC pluton: N1 = 184, N2 = 50, and N3 = 64; M1 = 36, M2 = 10, and M3 = 12.
CM pluton: N1 = 560, N2 = 20, and N3 = 172; M1 = 49, M2 = 3, and M3 = 19.

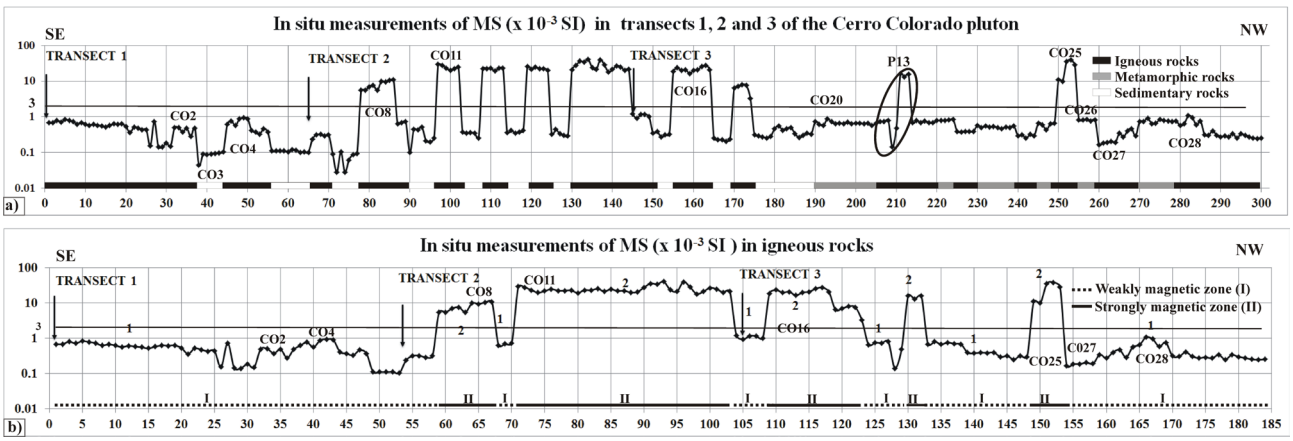

Figure 10. MS variations in outcrops of the CC pluton. a) Outcrops of igneous, sedimentary, and metamorphic rocks; b) outcrops of igneous rocks, in which vertical arrows indicate the start of each transect and P13 and circle indicate two groups of measurements in the same block of igneous rocks. 1 and 2 indicate groups of rocks. CO2 to CO28 indicate sample numbers.

content from 0.2% to 0.5% with a geometric mean of 0.3%, eU content from 0.8 to 2.0 ppm with a geometric mean of 1.4 ppm, and eTh content from 1.0 to 5.4 ppm with a geometric mean of 3.6 ppm (Table).

5. Discussion

5.1. Comparison of the CC and CM plutons

In the study area, the more basic igneous rocks are located in the CC pluton according to their highest values of MS (see maximum and geometric mean; Table) that indicate a high content of paramagnetic and ferromagnetic minerals. These rocks are mostly located in transect 2 (P2) (Figure 10), outside of the contact metasomatism zone (Figure 1). GS data also support this by identifying the igneous rocks of the CM pluton as more radioactive and therefore more acidic than those of the CC pluton.

The higher GS values in the final sections of the transects in the CM pluton and in the final section of transect 3 (P3) of the CC pluton (Figures 13 and 14) support the approach of higher acidity in the igneous rocks located near the center of the CM pluton. Also, the igneous rocks of this pluton show a larger geometric standard deviation (Figure

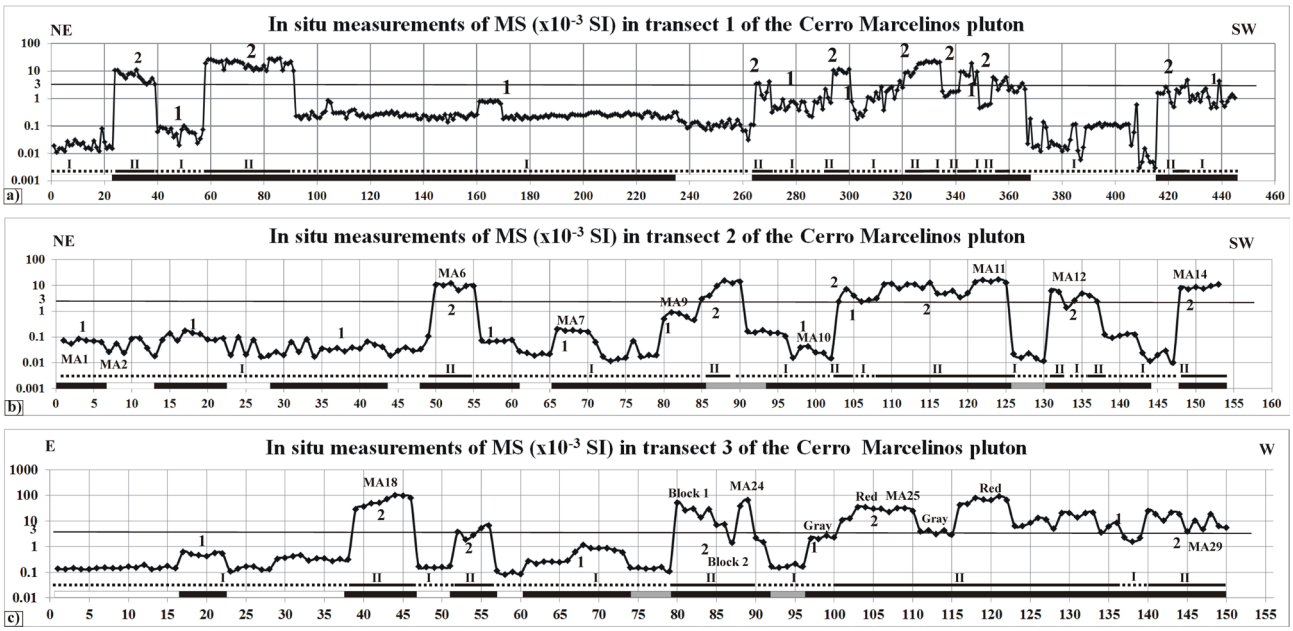

Figure 11. MS variations in outcrops of the CM pluton. a) Transect 1 (P1). b) Transect 2 (P2). c) Transect 3 (P3). Blocks 1 and 2 indicate blocks of igneous rocks. Gray and red indicate the color of the igneous rocks. MA1 to MA29 indicate samples numbers.

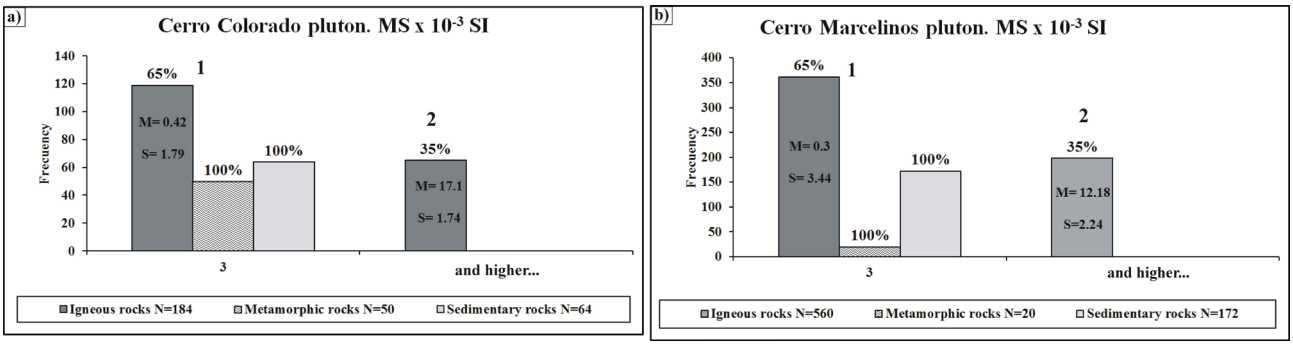

Figure 12. MS histograms of the three rock types in the plutons. a) CC pluton. b) CM pluton. 1 and 2 indicate groups of rocks according to the values of MS. Numbers above the bars of the histograms indicate the percent of the total number of measurements of MS in each type of rock. N indicates the number of observations in each rock type. M: Geometric mean. S: Geometric standard deviation.

12b), indicating greater heterogeneity regarding magnetic properties.

The lower geometric mean value of the eTh/eU ratio in the limestones of the CC pluton (Table) indicates greater proportions of uranium compared to thorium. This is possibly related to higher organic matter content in the host limestone of this pluton compared with the CM pluton.

5.2. Geological interpretation of the trends

5.2.1. Emplacement and metamorphism process

High and low values of MS and GS in all transects of both plutons (Figures 10, 11, 13, and 14) are related to the intercalations of limestones with igneous and metamorphic rocks. These intercalations are indicators of the emplacement process of the plutons. It is possible that intrusions utilized tectonic weaknesses as passageways of emplacement causing additional structural deformation (Figure 2a) and metamorphism of the host rocks.

The variability in MS values in the final section of transect 3 (P3) of the CC pluton (Figure 10), as well as the end of the three transects of the CM pluton (Figure 11), suggests emplacement of different igneous bodies formed during multiple stages of magmatic differentiation. In addition, it is possible that this variability, which indicates the destruction of magnetic minerals (e.g., magnetite), originally occurred in igneous rocks and was caused by said rocks' metamorphism (Clark, 1997). This approach is based on the location of the contact metasomatism zone, in the initial and intermediate section of transect 3 of the CC pluton (Figure 1).

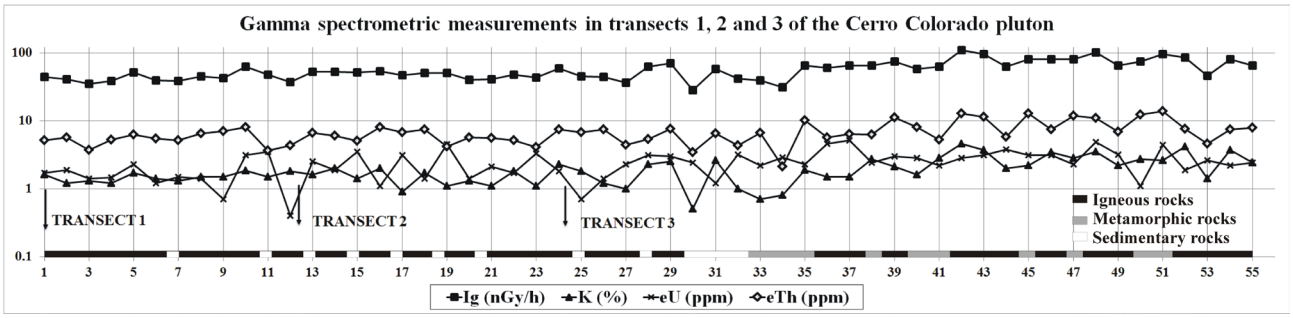

Figure 13. GS measurements in outcrops of the CC pluton. Vertical arrow indicates the start of each transect.

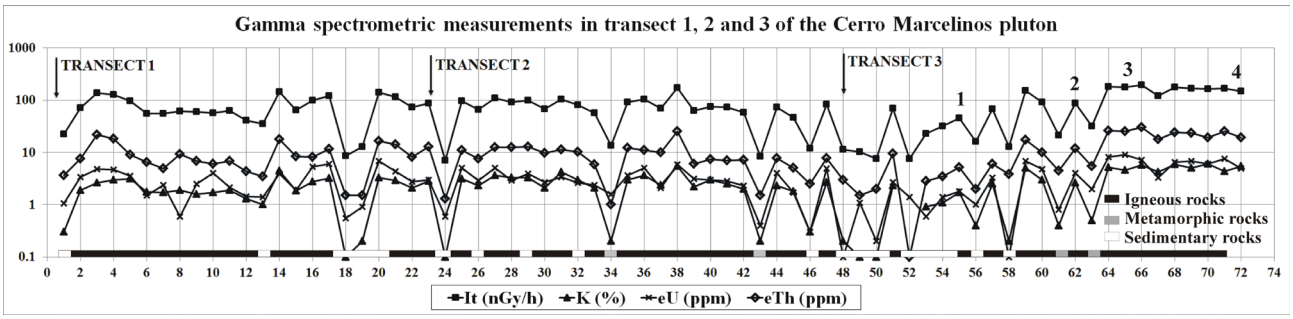

Figure 14. GS measurements in outcrops of the CM pluton. Vertical arrow indicates the start of each transect. 1, 2, 3, and 4 indicate locations of the MA18, MA24, MA25, and MA29 samples, respectively.

Outcrops of metamorphic rocks associated with both plutons differ markedly in their radioactive contents (Figure 13). Such differences indicate a contact metasomatism with differing degrees of alteration during emplacement of the plutons. The CC pluton has the more radioactive metamorphic rocks. These rocks are clearly more radioactive than the limestone host rocks. The increase of eU, eTh, and K concentrations in these metamorphic rocks is presumably related to the degree of metasomatism by magmatic fluids.

In the CM pluton, the metamorphic rocks are less radioactive than the limestone, suggesting that the original concentrations of uranium, thorium, and potassium have been depleted by alteration during the metamorphism. The effect of this last mentioned process has been reported in other research (e.g., Verdoya et al., 2001).

5.2.2. Weathering

Variations in the MS and GS values of the rocks in both plutons (Table; Figures 10, 11, 13, and 14) indicate changes in their mineralogical composition, which must be related to the conditions of origin and later alteration (Brimhal and Adams, 1969; Carmichael, 1989; Clark, 1997; Dickson and Scott, 1997; Oniku et al., 2008). In addition, in both plutons, the effects of contact metasomatism (Santiago-Carrasco et al., 2001; SGM, 2005) and intense weathering, mainly chemical, are observed (Figures 1, 2, and 3). Although the measurements of MS were performed on surfaces that do not show visible signs of weathering, the influence of leaching by hotter late magmatic fluids on the values of this physical property is not ruled out. Therefore, both processes can generate mineralogical change of the altered rocks, which affects their magnetic and radioactive properties. Chemical weathering can generate phases of secondary minerals (e.g., clays and iron oxides-hydroxides) from the alteration of primary phases (e.g., pyrite, feldspars, and micas). These secondary minerals can contribute to the increase or decrease of gamma radiation (Brimhal and Adams, 1969; Dickson and Scott, 1997) and MS values (Clark, 1997; Batista-Rodríguez et al., 2017). In particular, weathering leads to a loss of K in all rock types; however, for felsic igneous rocks, this process leads to a loss of uranium and thorium (Dickson and Scott, 1997). This process also may lead to oxidation of magnetite into hematite or goethite, thereby decreasing the MS of rocks (Tarling and Hrouda, 1993).

The low MS values of the igneous rocks located in the borders of the plutons are related to their high chemical weathering (Figure 2b) because this process causes the decrease of MS values (Clark, 1997; Batista-Rodríguez et al., 2017). This probably occurs because of the alteration of ferromagnetic minerals, producing minerals with lower saturation remanence such as the transformation of magnetite to hematite (Clark, 1997; Aydin et al., 2007). The coloration of the rocks in some outcrops is in

agreement with this scenario (Figures 2b, 2c, and 3c). At the borders of the plutons, the greatest tectonism of the rocks is also observed (Figures 2a and 3c), evidently related to emplacement.

5.2.3. Characteristics and alteration of the host sedimentary rocks

Differences in the eU, eTh, and K contents between outcrops of limestones (Figures 13 and 14) suggest variations in the degree of impurity and weathering of these rocks (Crick et al., 1997; Ellwood et al., 1999). High eTh content and sometimes K indicate that some of these limestones must be highly siliceous.

The values of MS recorded in the limestones (Table) suggest that their magnetic behavior is related to paramagnetic and sometimes ferromagnetic minerals identified by petrography, such as pyrite and iron oxides and hydroxides (Figures 5a and 5b; Figure 7c and 7d). These minerals increase the MS of the sedimentary rocks (Clark, 1997; Batista-Rodríguez et al., 2017). The origin of most of these minerals can be linked to the alteration of these rocks during the emplacement of the plutons. For example, in the limestones surrounding the CC pluton, pyrites with rectangular faces, i.e. with a cubic habitus, are observed (Figure 5b), showing the epigenetic origin of this mineral. It is possible that this mineral has been incorporated into the sedimentary rock through hydrothermal processes during the emplacement of the pluton (Batista-Rodríguez et al., 2017).

Limestones of the three transects in the CC pluton have different MS values, which suggest possible alterations of these rocks by various geological processes. Specifically, the limestones of transect 2 have higher MS than those of transect 1 (Figure 10), showing the greater intensity of the metasomatic process in the rocks of transect 2 and, therefore, greater enrichment in paramagnetic (e.g., epigenetic sulfides) and ferromagnetic minerals coming from the intrusion. Generally, it is observed that the host rocks close to the plutons have higher MS values than the same facies remote from the influence of these plutons (Batista-Rodríguez et al., 2017). This corroborates the observed effect of emplacement of the plutons on the magnetic composition of host rocks.

5.2.4. Magmatic differentiation

The increase of the eU, eTh, and K contents towards the center of both plutons indicates an increase of silica content and therefore a more acidic composition (Brimhal and Adams, 1969; Harenyama et al., 2006), which is evidence of the effect of magmatic differentiation (Oliveira et al., 2008). This process can occur by various mechanisms, such as fractional crystallization according to Bowen (1928) and assimilation (DePaolo, 1981; Freund et al., 2013). According to Dickson and Scott (1997), an increase in SiO_2 contents in the rocks causes an increase in uranium, potassium, and thorium contents, where Th is particularly diagnostic. In addition, Chiozzi et al. (2007) indicated that the concentration of uranium and potassium increases with the degree of magma differentiation. The increases in the three radioelements and the strong variations in the eTh content suggest a marked magmatic differentiation during the origin and emplacement of both plutons. According to Brimhal and Adams (1969), all three radioelements are excluded from the replacement of major element ions during the early crystallization of magma, which usually occurs via small quantities of silica, and are later incorporated into accessory minerals, such as monazite, xenotime, zircon, allanite, apatite, and sphene. Therefore, the GS data suggest that igneous rocks closer to the center of both plutons have high silica content, possibly associated with the later stages of the magmatic differentiation.

The greater variations of MS in igneous rocks show their high magnetic heterogeneities (Carmichael, 1989; Oniku et al., 2008). This is shown in image analysis of polished surfaces of intrusive rocks in both plutons (Figures 6, 8, and 9). Such variations are related to the effects of the magmatic differentiation process during the origin of the plutons.

The decrease in the values and MS variations within the plutons indicates that igneous rocks are less magnetic and more homogeneous in terms of the distribution of magnetic minerals. It is likely that the decrease of the MS values is related to the alteration of the minerals, primarily by the action of late magmatic or hydrothermal fluids, resulting in the oxidation of Fe oxides (Lapointe et al., 1986). In these zones, igneous rocks have lighter colorations (felsic rocks; Figures 8a, 8e, 8f, and 9), suggesting their origin in the later stages of magmatic differentiation, namely rocks highly enriched in felsic minerals and poor in ferromagnesian silicates, as well as iron oxides and hydroxides (Bowen, 1928). The decrease in MS values caused by the effects of tectonism and weathering is not considered because both processes are not well developed in this sector of the study area; therefore, MS can nevertheless be used as a magmatic differentiation index (Oliveira et al., 2008).

5.2.5. Classification of the igneous rocks

The eU, eTh, and K contents in igneous rocks of both plutons are analogous to the ranges recorded in intermediate-basic rocks in other regions of the world. These contents are typical of diorites and granodiorites (Dickson and Scott, 1997; Chiozzi et al., 2007), which outcrop in the study region according to Santiago-Carrasco et al. (2001) and SGM (2005).

Results from elsewhere have suggested that acid and intermediate intrusive rocks can be described as magnetic when MS values are higher than 10^{-3} SI and weakly magnetic when MS values are between 10^{-4} and 10^{-5} SI (Bouchez, 2000). In this study we classify the rocks from the two plutons into two groups based on the MS values

(group 1 with MS ≤ 3×10^{-3} SI and group 2 with MS > 3×10^{-3} SI). Using the spatial distribution of these groups, two magnetic zones in both plutons are delimited. Groups 1 and 2 are located in zones I and II, respectively. These zones are classified as weakly magnetic and strongly magnetic (I and II, respectively; see Figures 10 and 11). Zone II is mainly located inside the plutons and has rocks with MS controlled by ferromagnetic minerals, unlike zone I, in which MS is essentially related to paramagnetic minerals.

According to the MS values, the sedimentary and metamorphic rocks are included in the first group of igneous rocks (Figure 12) and, therefore, the magnetic carriers of these two rock types could be similar and dominated mainly by paramagnetic minerals.

Research carried out in other regions of the world uses the magnetic minerals of granitoids (granites, granodiorites, tonalities, etc.) to classify them into two series: magnetite and ilmenite (Ishihara, 1977; Ellwood and Wenner, 1981; Ishihara et al., 2000; Maulana et al., 2013). Magnetite and/or magnetite-ilmenite predominate in the magnetite series, whereas ilmenite and/or hemo-ilmenite prevail in the ilmenite series. Generally, the granitoids of the magnetite series have magnetite, ilmenite, and sulfides (e.g., pyrite, chalcopyrite, and pyrrhotite), whereas ilmenite and sulfides (e.g., pyrrhotite) are the principal magnetic minerals in the ilmenite series (Whalen and Chappell, 1988). In this research, the MS values and, therefore, the supposed carriers of the magnetization suggest that the igneous rocks of group 1 (MS ≤ 3×10^{-3} SI) belong to the ilmenite series and the rocks of groups 2 (MS > 3×10^{-3} SI) to the magnetite series (Ishihara, 1977; Maulana et al., 2013).

Unlike the CC pluton, in the CM pluton, there is an increase in MS values towards the interior where group 2 of the igneous rock predominates (Figure 11). This indicates greater magnetism and therefore the predominance of granitoids of the magnetite series in the last stages of the magmatic differentiation process.

5.3. Potential mineralization

The classification of igneous rocks into groups and their placement in one of the aforementioned series is of great importance for mineral exploration because of the mineralization types that can relate to the rocks of these series. According to Ishihara (1977) and Blevin and Chappell (1992), there is a clear correlation between the MS of granitoids and their associated mineralization. For example, Cu and Au are associated with the magnetite series, intermediate I-type granitoid suites. In the CC pluton, mineralizations of Cu, Au, Ag, Pb, and Zn are reported, related with sulfides originating from metasomatic processes. These mineralizations are located in the El Regalo and La Poderosa mines (SGM, 2005; González-Ramos et al., 2008). Alternatively, in the CM pluton, Cu and Fe mineralizations related to sulfides originating from metasomatic processes also are described in the La Buena Suerte and Marcelinos mines (Santiago-Carrasco et al., 2001; González-Ramos et al., 2008).

As zone II predominates the mineralized areas of the final section of the transects, it can be concluded that rocks of the magnetite series predominate this area of strongly magnetic igneous rocks. Therefore, the zones of granitoid of the magnetite series in both plutons (igneous rocks with MS > 3×10^{-3} SI) are zones of interest to locate and characterize mineralizations rich in Cu and Au, as well as other reported metals in these plutons. For this reason, it is possible to state that the magnetic zonation in both studied plutons can be used in future mineral exploration endeavors in these plutons and in other regions with igneous rocks.

6. Conclusions

The analysis of MS and GS suggests possible changes in the mineralogy of the igneous, sedimentary, and metamorphic rocks of the CC and CM plutons. These mineralogical changes are inferred to be related to the alteration that rocks undergo during the origin and emplacement of plutons. The alterations occur mainly by metamorphism and chemical weathering. The effect of weathering is more evident towards the border of the plutons. The differences between the radioactive contents in the outcrops of metamorphic rocks indicate a contact metasomatism with differing degrees of alteration during emplacement of the plutons. The host limestones show variations in the degree of impurity, which can be related to magnetic minerals incorporated during the intrusion process. Both physical properties suggest an increase in the degree of acidity towards the center of both plutons, indicating rocks most enriched in silica and possibly associated with the later stages of the magmatic differentiation process. Magnetic zones were defined in the plutons, associated with two groups of igneous rocks (group 1 with MS ≤ 3×10^{-3} SI and group 2 with MS > 3×10^{-3} SI). Group 1 is associated with the magnetite series and group 2 with the ilmenite series, which may be associated with mineralizations of mainly Au and Cu. Mainly, the magnetite series (group 2) delimited the more promising zones. Therefore, MS provides useful information regarding the internal magnetic zoning in the plutons. According to this analysis in the CM pluton, the granitoids of the magnetite series predominate in the last stages of the magmatic differentiation process, whereas in the CC pluton in the last stages of this process, the ilmenite series is present. This proposed zonation is an important indicator for guiding future exploration studies in comparable igneous terranes elsewhere.

Acknowledgment

We thank the Autonomous University of Coahuila and particularly the Higher School of Engineering for support of this research.

References

Aydin A, Ferré EC, Aslan Z (2007). The magnetic susceptibility of granitic rocks as a proxy for geochemical composition: example from the Saruhan granitoids, NE Turkey. Tectonophysics 441 (1-4): 85-95. doi: 10.1016/j.tecto.2007.04.009

Batista-Rodríguez J, Proenza-Fernández J, Rodríguez-Vega A, López-Saucedo F, Cázares-Carreón K (2017). Magnetic susceptibility and natural gamma radioactivity as indirect proxies for characterization of sandstones and limestones of the Sabinas basin. Geofizika 34: 19-43. doi: 10.15233/gfz.2017.34.6

Blevin PL, Chappell BW (1992). The role of magma sources, oxidation states and fractionation in determining the granite metallogeny of eastern Australia. Transactions of the Royal Society of Edinburgh. Earth Sciences 83 (1-2): 305-216. doi: 10.1017/S0263593300007987

Bouchez JL (2000). Magnetic susceptibility anisotropy and fabrics in granites. Comptes Rendus de l'Académie des Sciences-Series IIA - Earth and Planetary Science 330 (1): 1-14. doi: 10.1016/S1251-8050(00)00120-8

Bowen NL (1928). The Evolution of the Igneous Rocks. Princeton, NJ, USA: Princeton University Press.

Brimhal WH, Adams JAS (1969). Concentration changes of thorium, uranium and metals in hydrothermally altered Conway Granite, New Hampshire. Geochimica et Cosmochimica Acta 33 (10): 130-131. doi: 10.1016/0016-7037(69)90050-7

Carmichael RS (1989). Practical Handbook of Physical Properties of Rocks and Minerals. 1st ed. Boca Raton, FL, USA: CRC Press.

Chávez-Cabello G, Aranda-Gómez JJ, Iriondo-Perrones A (2009). Culminación de la Orogenia Laramide en la Cuenca de Sabinas, Coahuila, México. Boletín de la Asociación Mexicana de Geólogos Petrolero 54 (1): 78-89 (in Spanish).

Chiozzi P, Pasquale V, Verdoya M (2007). Radiometric survey for exploration of hydrothermal alteration in a volcanic area. Journal of Geochemical Exploration 93 (1): 13-20. doi: 10.1016/j.gexplo.2006.07.002

Clark DA (1997). Magnetic petrophysics and magnetic petrology: aids to geological interpretation of magnetic surveys. AGSO Journal of Australian Geology & Geophysics 17 (2): 83-103.

Crick RE, Ellwood BB, Hassani AE, Feist R, Hladil J (1997). Magnetosusceptibility event and cyclostratigraphy (MSEC) of the Eifelian-Givetian GSSP and associated boundary sequences in North Africa and Europe. Episodes 20 (3): 167-175. doi: epiiugs/1997/v20i3/004

DePaolo DJ (1981). Trace element and isotopic effects of combined wallrock assimilation and fractional crystallization. Earth and Planetary Science Letters 53(2): 189-202. doi: 10.1016/0012-821X(81)90153-9

Dickson BL, Scott KM (1997). Interpretation of aerial gamma ray surveys-adding the geochemical factors. AGSO Journal of Australian Geology & Geophysics 17 (2): 187-200.

Ellwood BB, Crick RE, El Hassani A (1999). The magnetosusceptibility event and cyclostratigraphy (MSEC) method used in geological correlation of Devonian rocks from Anti-Atlas Morocco. AAPG Bulletin 83 (7): 1119-1134. doi: 10.1306/E4FD2E8D-1732-11D7-8645000102C1865D

Ellwood BB, Wenner DB (1981). Correlation of magnetic susceptibility with 180/160 data in late orogenic granites of the southern Appalachian Piedmont. Earth and Planetary of Science Letter 54 (2): 200-202. doi: 10.1016/0012-821X(81)90003-0

Freund S, Beier C, Krumm S, Haase KM (2013). Oxygen isotope evidence for the formation of andesitic dacitic magmas from the fast-spreading Pacific-Antarctic Rise by assimilation-fractional crystallisation. Chemical Geology 347: 271-283. doi: 10.1016/j.chemgeo.2013.04.013

Goldhammer RK (1999). Mesozoic sequence stratigraphy and paleogeographic evolution of northeast Mexico. In: Bartolini C, Wilson JL, Lawton TF (editors). Mesozoic Sedimentary and Tectonic History of North-Central Mexico. 1st ed. Boulder, CO, USA: Geological Society of America, pp. 1-58. doi: 10.1130/0-8137-2340-X.1

González-Ramos A, Martínez-Ramos C, Izaguirre-Ramos MA, Barbosa-Luna D, Santiago-Carrasco B (2008). Carta geológico-minera Monclova G14-4. Coahuila y Nuevo León. Escala 1:250 000. Mexico City, Mexico: Servicio Geológico Mexicano (in Spanish).

Harenyama M, Tsuchiya N, Takeba M, Chida T (2006). Two dimensional measurement of radioactivity of granite rocks by photostimulated luminiscence technique. Geochemical Journal 34: 1-9.

Ishihara S (1977). The magnetite-series and ilmenite-series granitic rocks. Mining Geology 27 (145): 293-305. doi: 10.11456/shigenchishitsu1951.27.293

Ishihara S, Hashimoto M, Machida M (2000). Magnetite/ilmenite series classification and magnetic susceptibility of Mesozoic-Cenozoic batholiths in Peru. Resource Geology 50 (2): 123-129. doi: 10.1111/j.1751-3928.2000.tb00062.x

Lapointe P, Morris WA, Harding KL (1986). Interpretation of magnetic susceptibility; a new approach to geophysical evaluation of the degree of rock alteration. Canadian Journal of Earth Sciences 23 (3): 393-401. doi: 10.1139/e86-041

Lecoanet H, Léveque F, Segura S (1999). Magnetic susceptibility in environmental applications: comparison of field probes. Physics of the Earth and Planetary Interiors 115(3-4): 191-204. doi: 10.1016/S0031-9201(99)00066-7

Maulana A, Watanabe K, Imai A, Yonezu K (2013). Origin of magnetite- and ilmenite-series granitic rocks in Sulawesi, Indonesia: magma genesis and regional metallogenic constraint. Procedia Earth and Planetary Science 6: 50-57. doi: 10.1016/j.proeps.2013.01.007

Oliveira DC, Dall'Agnol R, Corrêa da Silva J, Costa de Almeida J (2008). Gravimetric, radiometric and magnetic susceptibility study of the Paleoproterozoic Redenção and Bannach plutons, eastern Amazonian Craton, Brazil: implications for architecture and zoning of A-type granites. Journal of South American Earth Sciences 25 (1): 100-115. doi: 10.1016/j.jsames.2007.10.003

Oniku SA, Osazuwa IB, Meludu OC (2008). Preliminary report on magnetic susceptibility measurements on rocks within the Zaria granite batholith, Nigeria. Geofizika 25 (2): 203-213.

Padilla RJ, Sánchez RJ (1986). Post-Paleozoic Tectonics of Northeast Mexico and its role in the evolution of the Gulf of Mexico. Geofísica Internacional 25 (1): 157-206.

Santiago-Carrasco B, Chiapa-García R, Martínez-Zárate EG (2001). Carta geológico-minera La Gloria G14-A62, Coahuila, Escala 1:50 000. Mexico City, Mexico: Servicio Geológico Mexicano (in Spanish).

Sewell CR (1968). The Candela and Monclova Belts of igneous intrusions, a petrographic province in Nuevo León and Coahuila, México (Abstract). In: Annual Meeting of the Geological Society of America, Abstract with Programs, p. 273.

SGM (2005). Carta geológico-minera Candela G14-A54, escala 1:50 000, estado de Coahuila. Mexico City, Mexico: Servicio Geológico Mexicano (in Spanish).

Silva PF, Henry B, Marques FO, Font E, Mateus A et al. (2008). Magma flow, exsolution processes and rock metasomatism in the Great Messejana–Plasencia dyke (Iberian Peninsula). Geophysical Journal International 175 (2): 806-824. doi: 10.1111/j.1365-246X.2008.03920.x

Tarling DH, Hrouda F (editors) (1993). The Magnetic Anisotropy of Rocks. 1st ed. London, UK: Chapman & Hall.

Verdoya M, Chiozzi P, Pasquale V (2001). Heat producing radionuclides in metamorphic rocks of the Brianeonnais-piedmont zone (Maritime Alps). Eclogae Geologicae Helvetiae 94 (2): 1-7. doi: 10.5169/seals-168890

Whalen JB, Chappell BW (1988). Opaque mineralogy and mafic mineral chemistry of I- and S-type granites of the Lachlan fold belt, southeast Australia. American Mineralogist 73: 281-296

Wilson JL (1990). Basement structural controls on Mesozoic carbonates facies in northeastern Mexico: a review. In: Tucker ME, Wilson JL, Crevello PD, Sarg JR, Read JF (editors). Carbonate Platforms, Facies, Sequences and Evolution. 1st ed. Ghent, Belgium: International Association of Sedimentologists, pp. 235-255. doi: 10.1002/9781444303834.ch9